PAPER • OPEN ACCESS

Techno-economic study on green hydrogen production and use in hard-to-abate industrial sectors

To cite this article: F Superchi *et al* 2022 *J. Phys.: Conf. Ser.* **2385** 012054

View the article online for updates and enhancements.

Techno-economic study on green hydrogen production and use in hard-to-abate industrial sectors

F Superchi[*]**, A Mati, M Pasqui, C Carcasci and A Bianchini**

Università degli Studi di Firenze, Department of Industrial Engineering, Via di Santa Marta 3, 50139 Firenze, Italy

[*]Corresponding author - francesco.superchi@unifi.it

Abstract. Replacing the bulk of grey hydrogen needed by industrial processes with a green one is one of the challenges of energy transition. In this study, the problem is analyzed from the perspective of a pre-determined amount of hydrogen to be delivered to hard-to-abate industries (steel mills and chemical industries) and produced by a wind farm converted or specifically installed for the scope. A hybrid configuration of the resulting energy system is figured out, considering a wind farm of twelve utility-scale turbines (2.3 MW each, for a total of 28 MW) to be coupled with alkaline-type electrolyzers, Li-Ion batteries and a hydrogen storage system. Moreover, it is assumed that the plant can also get energy grid in specific conditions, thus not producing a 100% green hydrogen in transitory periods. Specific point of strengths of the analysis are represented by the availability of several-year wind power production data, industrial performance data for the electrolyzers, whose model also accounts for performance degradation due to temperature, realistic operational constraints and variable efficiency. A battery aging model is also considered. A techno-economic analysis for different plant configurations is carried out with the aim of assessing how the systems performs form an economic and environmental point of view. Results show that is feasible to feed the plant with a constant hydrogen flow rate at a levelized cost of hydrogen (LCOH) of 4.95 €/kg with a green index (GI) around 64%, while a configuration that may reach higher GI (70%) presents a higher LCOH (5.26 €/kg).

1. Introduction

According to current estimates, the goals set by the European Union (EU) to reduce Greenhouse Gas (GHG) emissions [1] would imply a 32% increase in Renewable Energy Sources (RES) consumption by 2030, up to a 100% share in 2050 [2]. Within this framework, green hydrogen produced via water-electrolysis from RES is expected to play a key role in the decarbonisation of energy systems, thanks to its versatility as an energy vector able of converting, storing and releasing renewable energy for a wide range of applications (e.g., power to gas [3], [4]). While the deployment of large-scale hydrogen systems is globally gaining momentum as a mean to cope with RES unpredictability, hydrogen still finds presently its main application as an industrial feedstock for heavy industries such as refining, ammonia, steel and methanol production. World hydrogen demand for 2020 accounted for approximately 90 Mt, mostly produced via low-cost production methods namely Steam Methane Reforming (SMR), oxidation, and gasification, bearing in contrast the impressive environmental cost of around 900 Mt y^{-1} of CO_2 [5]. Concerning the deployment of a new hydrogen economy, the EU agenda has set some priorities, among which the first one is to decarbonise the sectors that are already using hydrogen like the chemical industry and industrial processes, i.e., the so-called *Hard-to-Abate* sectors. Such definition refers to any sector for which the transition is not straightforward due to a lack of dedicated technology or to its

prohibitive cost. From this perspective, hydrogen can represent a competitive alternative to the electric vector. In particular, the steel industry emerges as one of the top three contributors to CO_2 emissions, accounting for a remarkable share ranging between 4% and 7% of the global anthropogenic balance [6]; 70% of GHG emission in the sector are directly dependent on the use of carbon (coal or coke) both as a fuel and as a reductant [7]. A transition in ironmaking involving hydrogen has gained increasing attention and lies in the coupling of electrification and use of hydrogen as reductant. Several projects have recently been launched all over Europe for this purpose [8]–[11]. The basis of this approach is the use of Hydrogen Direct Reduction of Iron ore (HDRI) coupled with Electric Arc Furnace (EAF). This technology entails the potential of reducing steel production specific emissions in the EU by more than 35%, considering current grid emission levels [12]. In this context, innovative design and operation strategies for dedicated green hydrogen production system become key. To date, the coupling of green hydrogen hubs with different renewable energy sources has been addressed in literature, mainly considering solar photovoltaics (PV) and wind energy systems. The case for hydrogen production from dedicated wind farms is presented in several studies, both for offshore [13] and onshore configurations [14], analysing the interaction of different electrolysis technologies with storage systems and power grid connected plants. The most promising way to unlock the full potential of coupled wind energy and hydrogen production involves large-scale systems. Techno-economic feasibility of utility-scale applications is usually addressed via system optimization in terms of sizing and control having the lowest Levelized Cost Of Hydrogen (LCOH) as the key driver [15], [16]. However, there is a gap in the state of the art regarding the investigation of systems entirely dedicated to *Hard-to-Abate* sectors, designed to supply the needed amount of green hydrogen to guarantee current production standards at a sustainable environmental cost. This work in particular focuses on addressing the decarbonization of steel industry via a dedicated green hydrogen plant conceived as a hybrid configuration. A wind farm power plant is coupled with alkaline-type electrolyzers, Li-Ion batteries, hydrogen storage system, and an ancillary connection to the power grid. Building on a one-year power production dataset of a real wind farm, a series of 14508 different layout configurations and component sizes is evaluated through models that account for the real operating behavior of the considered technologies, such as electrolyzer thermal degradation and battery aging. Annual simulations are carried out for all the study cases, deriving the effect of some key size and performance parameters on two metrics, i.e., the standard LCOH and a newly proposed one represented by the percentage of renewable energy contained in the produced unit of hydrogen: Green Index (GI).

The present work is organized as follows: firstly, the reference case study is outlined in the materials and methods section followed by a description of the models adopted in the thermodynamic simulation of the system; the main economic parameters are presented as well. Then, the "results and discussion" paragraph reports the main outcomes obtained from the analysis of all possible system configurations in the given size range. Based on the above, two system layouts of interest are then identified for further economic evaluations: the one with the lowest LCOH value and a second one representing the best compromise between a high GI and a cost-effective system size. A detailed Net Present Value (NPV) sensitivity analysis of the two systems is therefore carried out and the incentive needed to make the most eco-friendly solution as attractive as the most cost-efficient one is quantified.

2. Materials and methods

The system considered in this study (Figure 1), is intended to produce a constant amount of hydrogen using an electrolyzer stack powered by a wind farm or by the power grid when wind production alone is not sufficient to satisfy the demand. The combined use of these two sources determines the final GI of the hydrogen produced, which is evaluated at the end of the simulation year as a comprehensive metric of the decarbonization potential of the system. With the aim of making the most of the wind farm production and reducing the amount of energy withdrawn from the grid, two types of storage can be included in the system: a battery, upstream of the electrolyzer stack, and hydrogen tanks, at the end of the production chain. A detailed description of each component is provided below.
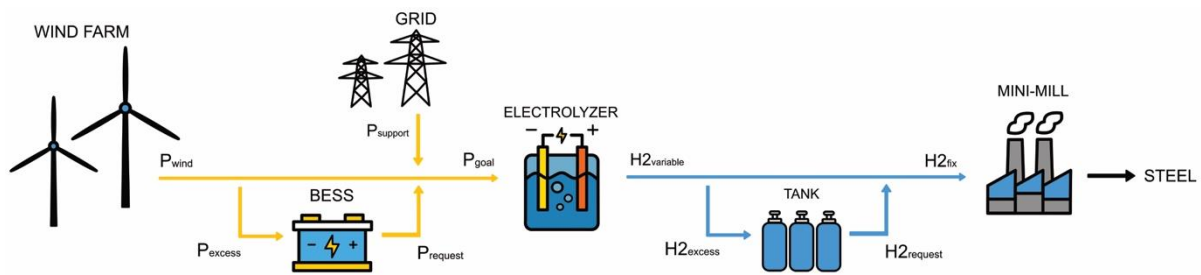
Figure 1. Hydrogen production system scheme

2.1. Reference case study

2.1.1 Steel mill and green hydrogen request. A steel mini-mill has been considered as the final consumer of green H_2 for this analysis. It is a new kind of industrial plant for steel manufacturing characterized by lower production volumes and greater versatility. In the steel production process, hydrogen can replace coke as reducing agent in a hydrogen direct reduction furnace to produce direct reduced iron (DRI). Then, the DRI is fed to the electric arc furnace (EAF) to produce emission free steel [17]. In this kind of plants, the EAF will likely be charged with equal shares of DRI and steel scrap to be recycled, thus requiring 25 kg (or 278 Nm^3) of hydrogen per ton of output steel [18]. New small-scale steel mills under development will have a relatively low annual yield down to 100 000 t/y [10], meaning that the daily production will settle around 274 tons of steel. Under these conditions, the daily hydrogen demand is approximately 76100 Nm^3, which corresponds to 3170 Nm^3/h. The commercial electrolyzer that is considered in this analysis, at rated conditions, produces 200 Nm^3/h per MW of electric power. Hence, to satisfy the hydrogen request it is required at least an installed electrolytic power of 16 MW.

2.1.2 Wind energy production. The renewable power fed into the electrolyzer is produced by a wind farm. The wind dataset utilized in this analysis is derived from real power production data of a utility-scale wind farm (WF) located in Greece, composed by six 2.3 MW onshore wind turbines. One year of data coming from the SCADA system of the farm was kindly provided by the owner of the system (Eunice Energy Group) with a time resolution of 10 minutes. For a capacity factor of around 30%, the number of equivalent working hours corresponds to 2660 h/year. After a preliminary analysis and cleaning of the dataset, power production was scaled up by a factor of 2 to meet appropriate power levels for the required H2 production, reaching a total nominal power of 28 MW. Figure 2 compares the power production output of the wind farm along the considered year (black line), with the required power level of 16 MW to produce the hydrogen fixed demand (red line). The mismatch between the production and the request is apparent and the potential benefit of an energy storage system can be argued.
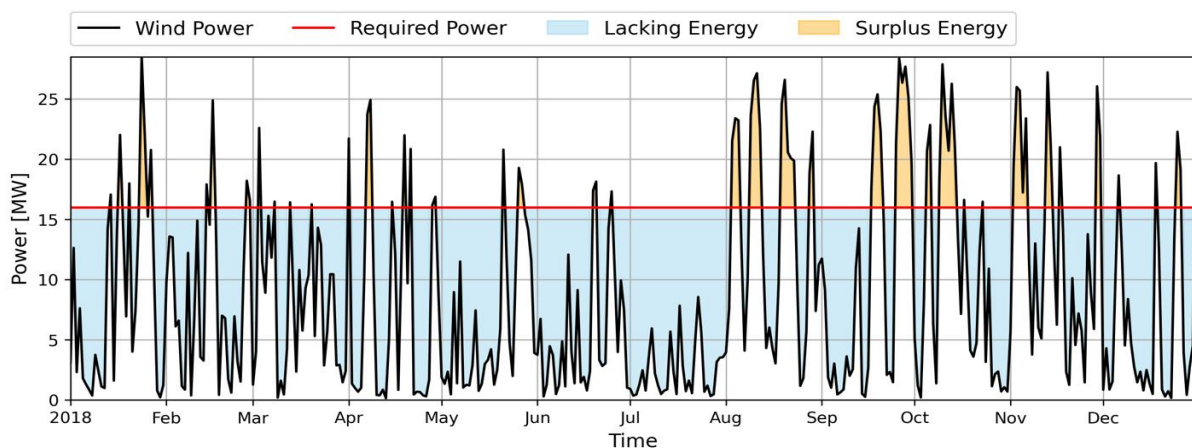

Figure 2. Power production of the WF and power request, highlight on lacking and surplus energy

2.2. Models

2.2.1 Electrolyzer. An original model of an alkaline electrolyzer calibrated on a commercial device produced by McPhy was employed to assess the hydrogen production capabilities of the system. Such model considers combinations of three commercial module sizes (1, 2 and 4 MW [19]) to reach the electrolytic power required by the simulation. Due to the intermittent operation that the module undergoes, the model considers the variation of the conversion factor $\varphi = H_{2,id}/(I_{id} \cdot V_{op})$, that characterizes the electrolyzer, i.e., the conversion efficiency from electric power input to green hydrogen output. The electric power required by the cell stack inside the electrolyzer module is given by the product of operating voltage and current, linked by a polarization curve. The model considers the effect of time and temperature: at each timestep, the model quantifies the voltage variation according to those effects. In actual high current stack technology, time degradation causes an increase in the required voltage per working hour while thermal degradation causes the same effect per each degree of cool down with respect to rated conditions. For a detailed analysis of those effect considered by the models see [20]. The model computes the electric power (P_{el}) that can be fed to the electrolyzer, according to the current wind power production and the availability of the battery or grid support. At each timestep, once the conversion factor is updated and the available power is estimated, the amount of hydrogen that the stack produces is computed as $H_2 = \varphi \cdot P_{el}$.

2.2.2 Battery. The battery model simulates the behaviour of a lithium-ion Battery Energy Storage System (BESS) and is based on a previous study by some of the authors [21]. The main considered parameters are the state of charge (SOC), limited to 15-95% to avoid harmful deep cycles, and the charging rate (C-rate), limited to full charge in 1 hour (1C) and full discharge in 2 hours (2C). The BESS represents a way to smooth the power fluctuations of the wind farm downstream the electrolyzer. According to the current needs (charging or discharging), at each timestep the SOC is computed and the charging and discharging efficiencies are affected by that. As a result of the technical limitations imposed to the parameters, the control algorithm corrects the trend of SOC, the C-rate and the power that is actually feasible to send to the electrolyzer from the battery. Thanks to the grid-supported operation, the discrepancy between the renewable power produced by wind farm (both direct and stored in BESS) and the goal power required to produce the set amount of green H_2 is provided by the electric grid.

2.2.3 Tank. A simplified model of a storage hydrogen tank has been developed to assess the convenience of including an energy storage downstream of the electrolyzer. This component allows the electrolyzer to produce a hydrogen stream higher than the user request if the power provided by the wind farm (or the battery) is high enough. The excess in hydrogen production is stored inside the tank and can be released when the production capability from RES fails to meet end-user demand. H_2 is considered to be stored at the same pressure level of the electrolyzer output (30 bar) and the tank capacity is always quantified referring to the gas volume at normal conditions (i.e., at 0 °C and 10^5 Pa) that can be contained. The model updates the amount of hydrogen stored inside the tank at each timestep and the grid support is activated only when the electrolyzer is not able to produce the required flow while the storage tank is empty. Figure 3 shows the trends of the battery SOC (blue line), the hydrogen tank SOC (green line) and the power extracted from grid (yellow line) during a month of operation for a configuration characterized by a 25 MW electrolyzer, a 30 MWh battery and a 150 kNm³ tank. The graph shows how the tank starts storing additional hydrogen when the battery is full, and an excess of power is available. Before the activation of the grid support, the battery and the tank release their content to support the constant hydrogen flow to the user.
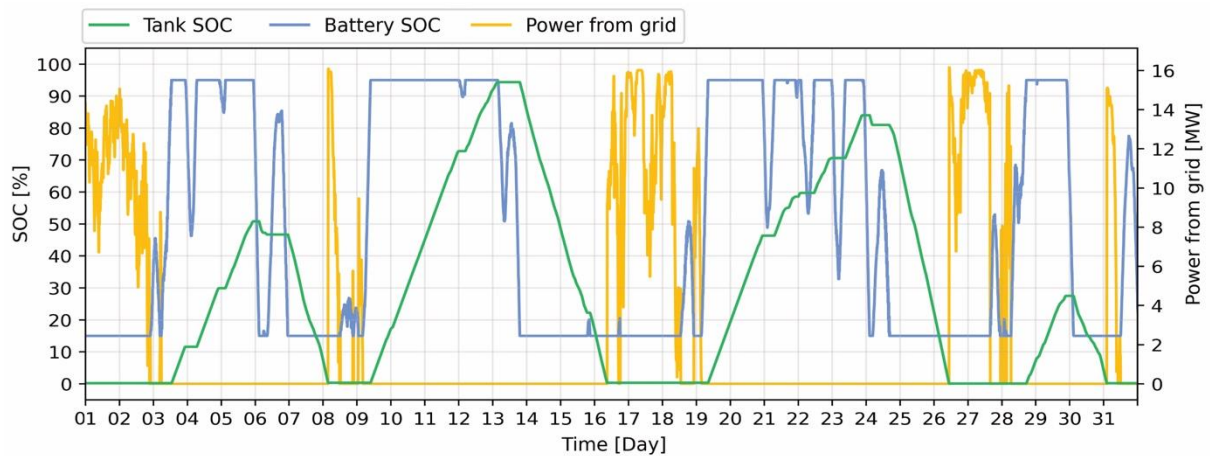
Figure 3. Tank and BESS SOC and electrical grid power request trend during a month of operation

2.3. Economic parameters

The LCOH is used to compare the economic viability of the different system configurations proposed. It represents the average revenue per unit of generated hydrogen that would be required to recover the costs of the system installation and operation during a lifetime (lt), assumed equal to 20 years. LCOH is calculated with equation (*1*); i is the interest rate set at 6%; CAPEX is the sum of the capital expenditures and OPEX is the sum of the operational expenditures, calculated with prices in Table 1. A specific lifetime is considered for each component, after which the cost for the substitution is included in the OPEX.

(1)

$$LCOH = \frac{\mathrm{i} \cdot \frac{(i+1)^{lt}}{(i+1)^{lt}-1} \cdot CAPEX + OPEX}{H_{2\ prod}}$$

Table 1. CAPEX and OPEX of components

Component	CAPEX	OPEX	Lifetime
Electrolyser	650 €/kW [22]	2.75% I_0 €/y [22]	10 years
Battery	117 €/kWh [23]	2.5% I_0 €/y [24]	10 years
H_2 Tank (30 bar)	460 €/kg [22], [25]	1% I_0 €/y [22]	20 years
WF electricity	-	36 €/MWh [23]	-
Grid electricity	-	108 €/MWh [26]	-

After using LCOH to evaluate the best system configurations, the net present value (NPV) of the system is calculated. Its evolution over years (y) allows to evaluate the type of the investment considering parameters such as payback time and profitability index. By doing this, different hydrogen sales prices (H_{price}) are assumed starting from H_{price} = LCOH. NPV_y is calculated with equation (*2*), considering as cash flow the revenues from selling the hydrogen at the assumed price, minus OPEX

(2)

$$NPV_y = NPV_{y-1} + (H_{2\ prod,y} \cdot H_{price} - OPEX_y)/(1+i)^y$$

2.4. Green Index

Since the envisioned system processes electricity from both the wind farm and the power grid, it is important to determine the percentage of "green" electricity that is turned into hydrogen. The Green Index (GI) is computed as the ratio between the electrical energy coming from renewables and the total energy converted into hydrogen $GI = (En_{WF} + 0.36 * En_{grid})/En_{tot}$. Referring to the Italian electricity mix, the renewable share of grid electricity (En_{grid}) is also taken in to account in the analysis, representing 36% of the total [27].

3. Results and discussion

This section presents the techno-economic assessment of the hydrogen production system considering different combinations of storage and electrolyzer stack sizes. Building on a dataset of 14508 different modelled configurations, the main results are hereafter presented. Electrolyzer stacks with a nominal power ranging from a base case of 16 MW (minimum required to meet H_2 constant demand) to a maximum of 28 MW (nominal power of the WF) were considered in the parametric analyses. First, a system without any storage is considered as the baseline scenario. Then, the possible advantages of storage systems are discussed.

Without any storage, the coupling of a 16 MW electrolyzer with the WF can feed hydrogen to the steel mill with a GI of 62.77%. In this case, only the instantaneous power that the wind farm produces can be exploited by the electrolyzer modules, and the electrical grid needs to satisfy the power gap when the WF production is lower than 16 MW. Hydrogen produced in this way has a LCOH of 4.97 €/kg, in line with current market prices of green H_2 [28] . Table 2 reports the main technical assumptions and capacity ranges considered for each component of the system.

Table 2. Technical assumptions of the main components of the system

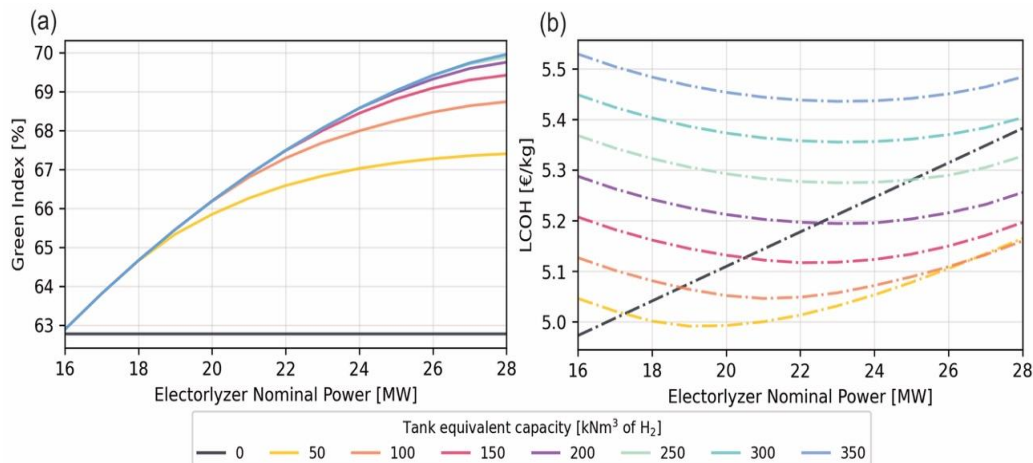| Component	Technical assumptions	Capacity range
Electrolyzer	Variable Temperature (71°C nominal) Variable Voltage (1.91V initial) 200 Nm^3/MWh	16-28 MW
Battery	15-95% SOC SOC dependent efficiency	0-30 MWh
H_2 Tank	0-100% SOC 30 bar	0-350 kNm^3

3.1. Hydrogen Tank

Figure 4. GI (a) and LCOH (b) varying electrolyzer nominal power and tank capacity, no BESS installed

Figure 4 shows the effect of the tank and electrolyzer size variation on the final LCOH (Figure 4 (a)) and GI (Figure 4 (b)). Tanks able to store from 0 to 350 kNm^3 of H_2 were considered for the analysis. When no tank is installed in the system (black lines), it appears unreasonable to power the electrolyzer modules at more than 16MW since there is no possibility of storing the produced hydrogen exceeding the steel mill demand. In this context, an increase in electrolytic power results in a linear increase in the LCOH without any gain for the GI parameter. On the other hand, when a storage system is present, it is convenient to install a higher capacity electrolyzer stack that may follow the power production peaks of the wind farm. Larger electrolyzer sizes coupled with high storage tank capacities result in a GI increase from 63% to 70%. Above a certain tank size, the increment in GI becomes negligible with respect to the

increase in installation costs: storage capacities higher than 200 kNm^3 of H$_2$ do not result in a sensible increment in the GI (ca. 0.1%) while inevitably determine an LCOH increase of 10 c€/kg on average. Figure 4 (b) shows minimums in LCOH because of the trade-off between higher initial investment and lower hydrogen purchase costs: installing a higher electrolyzer power allows to buy more electricity from the wind farm and less from the grid, thus reducing the total costs of producing hydrogen. To this end, a bigger tank is also needed to store the hydrogen not immediately used by the steel mill. The minimum shifts towards higher electrolyzer sizes when the tank capacity increases because an electrolyzer configuration that can process higher peak power levels better exploits bigger tanks. Figure 4 (b) also shows that the configuration without tank is the cheapest and will be thus analyzed in further detail in the following section.

3.2. Battery Energy Storage System (BESS)

Figure 5 shows the effect of BESS presence on the LCOH and GI of the produced H$_2$. Since no tank is present, only an electrolyzer with a nominal power of 16 MW was considered, together with a BESS capacity ranging from 0 to 30 MWh. The green line shows that this solution can increase the GI of more than 2 percentage points: from 62.78% with no BESS up to 65.13% when the largest considered storage capacity is installed. BESS also allows to increase the exploitation of the cheaper electric power coming from the WF, and this results in a decrease of the final LCOH for small battery sizes: the minimum of the LCOH curve corresponds to a BESS capacity of 8 MWh. For larger BESS, the LCOH rises again because the higher installation cost is no longer balanced by a significant increase in RES exploitation.
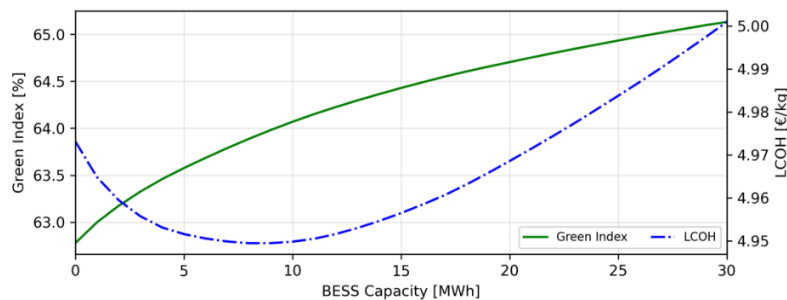

Figure 5. LCOH and GI varying BESS Capacity, no Tank installed

3.3. Combined system

3D plots in Figure 6 show a comprehensive overview of the combined effect of the two considered storage technologies (BESS and tank) on the LCOH (Figure 6 (a)) and GI (Figure 6 (b)), for different combinations of electrolyzer power and storage sizes. The size ranges defined for the parametric analysis are hereafter summarized: BESS 0-30 MWh, tank 0-350 kNm^3 and electrolyzer 16-28 MW.
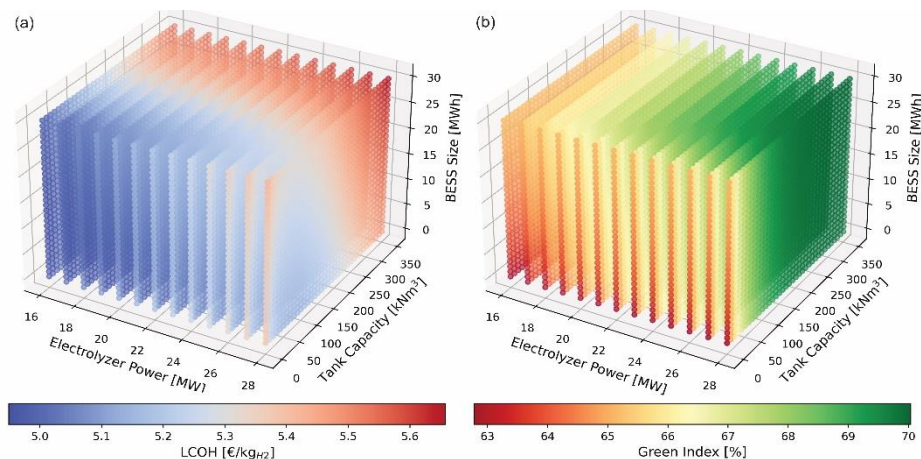

Figure 6. LCOH (a) and GI (b) indicators varying BESS Capacity, Tank Capacity and Electrolyzer Power

The LCOH zones in Figure 6 (a) show that configurations with a small tank result in the lowest LCOH: the combination of a 8 MWh BESS, no tank and a 16 MW electrolyzer is the most convenient one in economic terms. Larger tanks inevitably have a negative impact on the LCOH but, when paired with high power electrolyzers, may balance the higher installation cost: the last plane in Figure 6 (a) 28 MW electrolyzer, is convenient to add a tank storage with a capacity around 200 kNm^3 to store the H$_2$ excess produced during WF power production peaks. When the tank storage is present, the addition of BESS leads to an increase in the LCOH, since the best compromise between the higher exploitation of the renewable power and the initial investment for the storage system is reached yet considering the tank. Figure 6 (b) shows that larger H$_2$ tanks, paired with electrolyzer modules with a large nominal power, is the most effective way to increase the GI of the final product: from less than 63% when the tank is not present, up to 70% when a large tank is installed. When this solution is applied, the positive contribution on GI of a BESS system becomes negligible. Overall, the combination of large sizes of the two kinds of storage systems results ineffective both in economic and environmental terms.
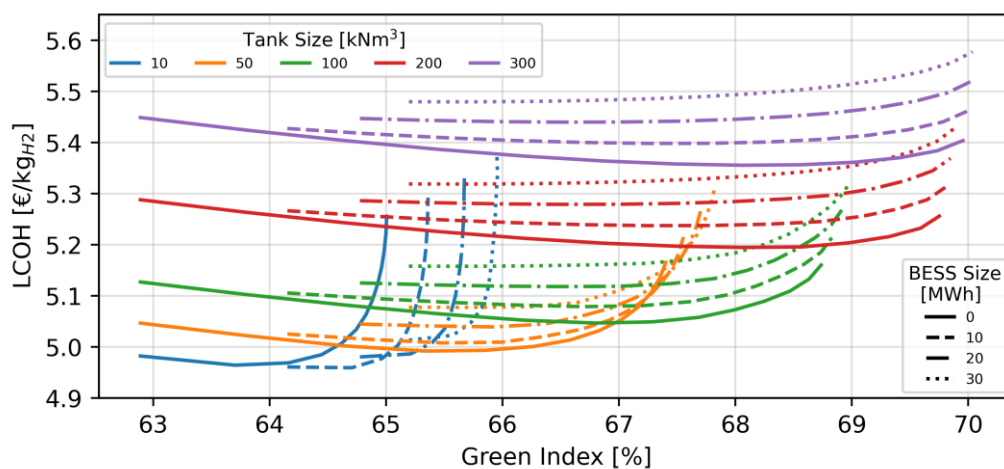

Figure 7. LCOH value over GI varying BESS and tank size.

Figure 7 helps getting a better interpretation of the discussed results by presenting the different behaviour of LCOH and GI indexes when varying both the tank and the BESS size included in the system. It is apparent how the influence of a BESS size variation on the performance is more prominent at low tank capacities, affecting both the economic and the environmental score (i.e., plotted lines for 10 kNm^3 storage system). On the other hand, for higher tank size values, it decreases its positive effect ending up to negatively impact solely the economic results due to higher initial investment costs for the oversized battery. It is also interesting to notice how the beneficial contribution of tank size variation on the GI ceases to be significant after the value of 200 kNm^3. Up to this value, curves of different colours visibly shift to the right as the size increases, thus showing better performance for the GI, thereafter the translation becomes vertical, presenting only a significant increase in LCOH compared to a negligible increase in GI. This behaviour, as already mentioned in section 3.1, underpins the choice of the second of the two configurations defined for the economic analysis as optimal for the GI factor.

3.4. Incentives evaluation on green hydrogen

Figure 8 (a) shows the net present value (NPV) trend in a period of 20 years for two configurations: the most favorable in economic terms (blue lines) and a system layout identified as the best solution for the highest GI values (green lines) as anticipated in section 3.2. Four different selling prices were considered for the produced H$_2$: 5.0, 5.1, 5.2 and 5.3 €/kg. The first configuration is characterized by the absence of a hydrogen tank, an electrolyzer size of 16 MW and an 8 MWh capacity battery. Such combination yields a GI of 63.88% and an LCOH of 4.95 €/kg. Even considering the lowest selling price, this configuration allows to recover the initial investment after 16 years, decreased to 7 years in the highest selling price scenario. The second configuration involves a large tank able to store 200 kNm^3 of H$_2$ and

an electrolyzer power of 28 MW, BESS capacity is kept to 0 MWh. Due to the larger size of the components, the investment cost of the second configuration is more than doubled compared to the first one. This is reflected in a higher LCOH of 5.26 €/kg but also in a higher GI of 69.75%. From the plot it is possible to derive that the "green" configuration can reach the revenues of the most economically effective one if the selling price of hydrogen is ~0.3 €/kg higher, corresponding to the difference between the two LCOH values. The NPV trend discontinuity occurring after 10 years of operation is due to the imposed replacement of the technologies that have reached the end of their specified lifetime (i.e. electrolyzer stack and battery).
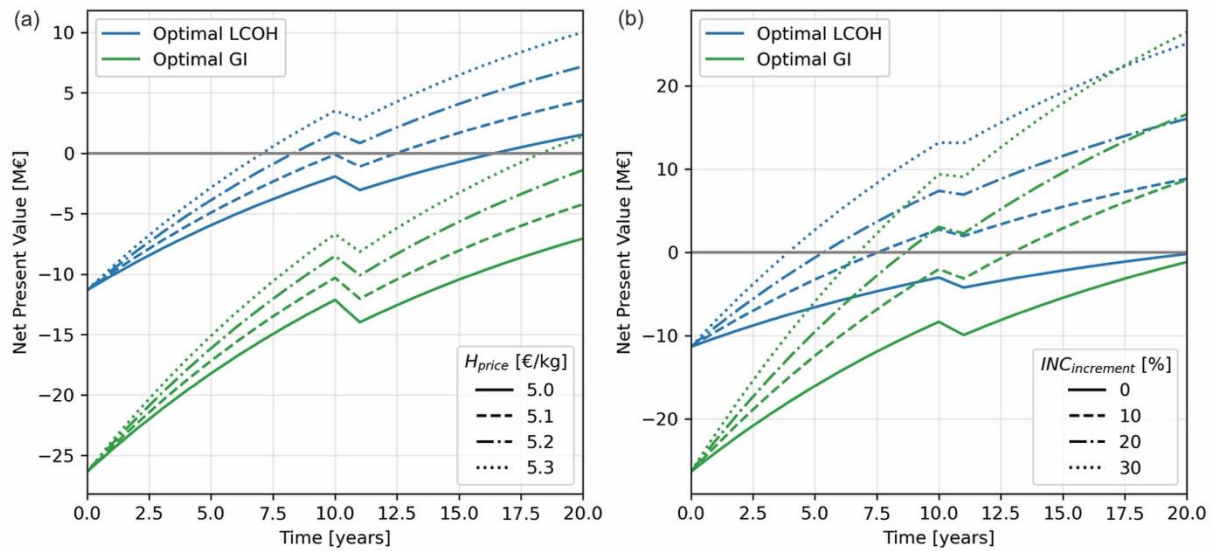

Figure 8. NPV evolution (a) and Incentive comparison (b) for optimal LCOH and GI configuration.

Compared to the current market price of grey hydrogen (~2 €/kg [28]), green hydrogen is still not economically competitive. A suitable strategy to boost the penetration of such decarbonized fuel could be based on incentives that reward producers on the percentage of green hydrogen on their final product (e.g., the GI). A hypothetical "green rewarding" policy is summarized by equation (3): to the current market price of grey hydrogen ($P_{H2\ market}$) is added an incentive (x_{inc}) proportional to the GI.

$$P_{H_2\ green} = P_{H_2\ market} + x_{inc} \cdot GI$$

(3)

Figure 8 (b) compares the NPV evolution of the two configurations considered before. Due to proposed incentives, this time the final selling price is different between the two and higher for the "green" configuration. Four incentives levels were considered, starting from the incentive that allows the most economically convenient configuration to recover the investment (4.6 €/kg). When it is incremented by 20% or more, the "green" configuration becomes more profitable than the first one. This analysis gives an idea on the magnitude of incentive that could push investors to install storage technologies in this kind of systems to increase the penetration of the renewable source and, consequently, the GI of the final hydrogen mix thus allowing for a significative decarbonization of the steelmaking industry.

4. Conclusions

The aim of this work was to assess the techno-economic feasibility of producing a constant flow of hydrogen needed to match the demand of newly conceived and potentially carbon-free steelmaking process relying on green hydrogen as a reductant (EAF-DRI). A hybrid operation of an alkaline electrolyzer stack was considered modeling the exploitation of a locally available RES (wind energy) supported by a grid connection to extract power from the grid when the local energy production is not sufficient. Results show that the implementation of a storage system allows for a better exploitation renewable energy, thus leading to lower production prices of the final product and higher percentages of green fuel. The best combination in economic terms derives from the pairing of a BESS with an

electrolyzer stack characterized by the minimum power level required. The lowest estimated LCOH by this kind of combinations is around 4.95 €/kg, in line with green H_2 prices. The combination of a hydrogen tank storage coupled with electrolyzers with higher power was instead proved as the most effective way to improve the GI in the final hydrogen mix, up to 70% with large tanks. However, the parametric analysis has shown that, for tank sizes higher than 200 kNm^3, there is no sufficient gain in GI to justify the higher initial investment. Outcomes of the economic analysis have shown that, if the hydrogen produced with the cheapest configuration is sold at 5 €/kg, the investment can be recovered in around 16 years. Moreover, an incentive-driven scenario was also explored to assess the magnitude of the subsidy that would make those configurations that reach higher GI competitive: if the green part is subsidized more than 5.5 €/kg, configurations with large storages can become competitive. Future work will explore scenarios with different final hydrogen requests. In addition, a better assessment of the steelmaking process could be carried out to account also for the electric consumption from the electric arc furnace. In that case, it could be possible to assess the share of renewables in the overall final energy consumption, thus quantifying accurately the sustainability of steel production in a decarbonized economy.

Bibliography

[1]   European Parliament, "Regulation (EU) 2021/1119 of the European Parliament and the Council of 30 June 2021 establishing the framework for achieving climate neutrality and amending Regulations (EC) No 401/2009 and (EU) 2018/1999 ('European Climate Law')," *Off. J. Eur. Union*, vol. 64, no. 7, pp. 1–17, 2021, [Online]. Available: https://eur-lex.europa.eu/legal-content/EN/TXT/PDF/?uri=OJ:L:2021:243:FULL&from=EN.

[2]   EU, "Directive (EU) 2018/2001 of the European Parliament and of the Council on the promotion of the use of energy from renewable sources," *Off. J. Eur. Union*, vol. 2018, no. L 328, pp. 82–209, 2018.

[3]   C. van Leeuwen and M. Mulder, "Power-to-gas in electricity markets dominated by renewables," *Appl. Energy*, vol. 232, pp. 258–272, Dec. 2018, doi: 10.1016/J.APENERGY.2018.09.217.

[4]   I. A. Gondal, "Hydrogen integration in power-to-gas networks," *Int. J. Hydrogen Energy*, vol. 44, no. 3, pp. 1803–1815, Jan. 2019, doi: 10.1016/J.IJHYDENE.2018.11.164.

[5]   "Hydrogen – Analysis - IEA." https://www.iea.org/reports/hydrogen (accessed Jun. 08, 2022).

[6]   L. Cozzi and T. Gould, "World Energy Outlook 2021," *IEA Publ.*, pp. 1–386, 2021, [Online]. Available: www.iea.org/weo.

[7]   "The net-zero transition for hard-to-abate sectors | McKinsey." https://www.mckinsey.com/business-functions/sustainability/our-insights/sectors-are-unevenly-exposed-in-the-net-zero-transition (accessed Jun. 09, 2022).

[8]   "SSAB is taking the lead in decarbonizing the steel industry." https://www.ssab.com/en-gb/fossil-free-steel (accessed Jun. 09, 2022).

[9]   "H2FUTURE PROJECT - Startseite." https://www.h2future-project.eu/ (accessed Jun. 09, 2022).

[10]   "Hydrogen-based steelmaking to begin in Hamburg | ArcelorMittal." https://corporate.arcelormittal.com/media/case-studies/hydrogen-based-steelmaking-to-begin-in-hamburg (accessed Jun. 09, 2022).

[11]   "GrInHy2.0 - GrInHy 2.0: Green Industrial Hydrogen 2.0." https://www.green-industrial-hydrogen.com/ (accessed Jun. 09, 2022).

[12]   A. Bhaskar, M. Assadi, and H. N. Somehsaraei, "Decarbonization of the iron and steel industry with direct reduction of iron ore with green hydrogen," *Energies*, vol. 13, no. 3, pp. 1–23, 2020, doi: 10.3390/en13030758.

[13]   V. N. Dinh, P. Leahy, E. McKeogh, J. Murphy, and V. Cummins, "Development of a viability assessment model for hydrogen production from dedicated offshore wind farms," *Int. J. Hydrogen Energy*, vol. 46, no. 48, pp. 24620–24631, Jul. 2021, doi: 10.1016/J.IJHYDENE.2020.04.232.

[14]   B. Olateju, A. Kumar, and M. Secanell, "A techno-economic assessment of large scale wind-

hydrogen production with energy storage in Western Canada," *Int. J. Hydrogen Energy*, vol. 41, no. 21, pp. 8755–8776, 2016, doi: 10.1016/j.ijhydene.2016.03.177.

[15]   S. McDonagh, S. Ahmed, C. Desmond, and J. D. Murphy, "Hydrogen from offshore wind: Investor perspective on the profitability of a hybrid system including for curtailment," *Appl. Energy*, vol. 265, no. February, p. 114732, 2020, doi: 10.1016/j.apenergy.2020.114732.

[16]   Y. Jiang, Z. Deng, and S. You, "Size optimization and economic analysis of a coupled wind-hydrogen system with curtailment decisions," *Int. J. Hydrogen Energy*, vol. 44, no. 36, pp. 19658–19666, 2019, doi: 10.1016/j.ijhydene.2019.06.035.

[17]   A. Bhaskar, R. Abhishek, M. Assadi, and H. N. Somehesaraei, "Decarbonizing primary steel production : Techno-economic assessment of a hydrogen based green steel production plant in Norway," *J. Clean. Prod.*, vol. 350, p. 131339, May 2022, doi: 10.1016/J.JCLEPRO.2022.131339.

[18]   V. Vogl, M. Åhman, and L. J. Nilsson, "Assessment of hydrogen direct reduction for fossil-free steelmaking," *J. Clean. Prod.*, vol. 203, pp. 736–745, 2018, doi: 10.1016/j.jclepro.2018.08.279.

[19]   "Large | McPhy." https://mcphy.com/it/apparecchiature-e-servizi/elettrolizzatori/large/?cn-reloaded=1 (accessed Jun. 27, 2022).

[20]   F. M. F. F. Superchi, F. Papi, A. Mannelli, F. Balduzzi, A. Bianchini, "Development of a Reliable Simulation Framework for Techno-economic Analyses on Green Hydrogen Production from Wind Farms Using Alkaline Electrolyzersitle," 2022.

[21]   A. Mannelli, F. Papi, G. Pechlivanoglou, G. Ferrara, and A. Bianchini, "Discrete Wavelet Transform for the Real-Time Smoothing of Wind Turbine Power Using Li-Ion Batteries," *Energies 2021, Vol. 14, Page 2184*, vol. 14, no. 8, p. 2184, Apr. 2021, doi: 10.3390/EN14082184.

[22]   J. Gorre, F. Ruoss, H. Karjunen, J. Schaffert, and T. Tynjälä, "Cost benefits of optimizing hydrogen storage and methanation capacities for Power-to-Gas plants in dynamic operation," *Appl. Energy*, vol. 257, p. 113967, Jan. 2020, doi: 10.1016/J.APENERGY.2019.113967.

[23]   IRENA, "Power Generation Costs 2020," 2021. doi: 10.1088/1751-8113/44/8/085201.

[24]   W. Cole, A. W. Frazier, and C. Augistine, "Cost Projections for Utility-Scale Battery Storage: 2021 Update," *Natl. Renew. Energy Lab.*, no. June, p. 21, 2021, [Online]. Available: www.nrel.gov/publications.

[25]   S. Kharel and B. Shabani, "Hydrogen as a long-term large-scale energy storage solution to support renewables," *Energies*, vol. 11, no. 10, 2018, doi: 10.3390/en11102825.

[26]   "ARERA - Prezzi finali dell'energia elettrica per i consumatori industriali - Ue a Area euro." https://www.arera.it/it/dati/eepcfr2.htm (accessed Jun. 07, 2022).

[27]   Terna, "Comunicato Stampa: NEL 2021 DECISO RECUPERO DEI CONSUMI ELETTRICI," pp. 2020–2021, 2021.

[28]   A. Ajanovic, M. Sayer, and R. Haas, "The economics and the environmental benignity of different colors of hydrogen," *Int. J. Hydrogen Energy*, 2022, doi: 10.1016/J.IJHYDENE.2022.02.094.